Eur Radiol
DOI 10.1007/s00330-010-1852-1

ULTRASOUND

**Katsutoshi Sugimoto**
**Junji Shiraishi**
**Fuminori Moriyasu**
**Shigeki Ichimura**
**Ryo Metoki**
**Kunio Doi**

# Analysis of intrahepatic vascular morphological changes of chronic liver disease for assessment of liver fibrosis stages by micro-flow imaging with contrast-enhanced ultrasound: preliminary experience

Received: 12 March 2010
Revised: 10 May 2010
Accepted: 24 May 2010


**Electronic supplementary material** The online version of this article (doi:10.1007/s00330-010-1852-1) contains supplementary material, which is available to authorized users.

K. Sugimoto (✉) · F. Moriyasu · S. Ichimura · R. Metoki
Department of Gastroenterology and Hepatology,
Tokyo Medical University,
6-7-1 Nishishinjuku, Shinjuku-ku, Tokyo, 160-0023, Japan
e-mail: sugimoto@tokyo-med.ac.jp
Tel.: +81-3-33426111
Fax: +81-3-53816654

K. Sugimoto · J. Shiraishi · K. Doi
Kurt Rossmann Laboratories for Radiologic Imaging Research,
Department of Radiology,
The University of Chicago,
Chicago, IL, USA

J. Shiraishi
School of Health Sciences,
Kumamoto University, Kumamoto, Japan

**Abstract** *Objective* To assess morphological vascular changes due to an increase in liver fibrosis by using micro-flow imaging (MFI) of contrast-enhanced ultrasound. *Methods* MFI was performed in 47 patients who underwent liver biopsy, and in 10 normal cases. For 27/57 cases, we performed MFI twice in order to assess the reproducibility of the examination, thus yielding a total of 84 examinations. Seven physicians interpreted each case individually by assigning confidence levels for the presence or absence of three imaging features that were related to alteration of portal vein morphology: angle widening, tapering/interruption and tortuosity. *Results* Pearson's correlation coefficient between the average rating scores based on tortuosity and the histological fibrosis stage was 0.806 ($p<0.001$). The diagnostic accuracy of the average area under the ROC curve, which was estimated by use of the confidence levels of tapering/interruption, tortuosity and angle widening, was 0.964 for F1 vs. F2–4, 0.968 for F1–2 vs. F3–4 and 0.910 for F1–3 vs. F4. The average correlation coefficient between the ratings on different images from the same patients was 0.838. *Conclusion* Assessment of morphological intrahepatic vascular changes on MFI may be useful for grading liver fibrosis.

**Keywords** Ultrasound · Contrast media · Micro-flow imaging · Liver fibrosis · Vascular morphology

## Introduction

The definition of cirrhosis remains based on morphology, described by a working party for the World Health Organisation (WHO) in 1978 as "a diffuse process characterized by fibrosis and the conversion of normal liver architectures into structurally abnormal nodules" [1]. Nodularity is a prerequisite for the definition. However, intrahepatic vascular changes associated with cirrhosis are also an important component of the pathophysiology and progression of cirrhosis.

Some studies were performed to radiologically and pathologically investigate intrahepatic vascular changes of chronic liver disease [2, 3]. However, to the best of our knowledge, there has been no report correlating small portal vein branch morphologic changes as shown by contrast-enhanced ultrasound (CEUS) with the degree of liver fibrosis.

CEUS is a dynamic real-time examination performed with intravascular microbubble contrast agents. A new technical advancement in CEUS, micro-flow imaging (MFI; Toshiba, Otawara, Japan) known as maximum

Published online: 23 June 2010

intensity projection (MIP) imaging, much like time-lapse photography, integrates information about the microbubble pathway between frames and thus allows one to observe lesional vessels in exquisite detail, with the potential to show both their morphology and their direction of filling [4–6]. Moreover, microbubbles for ultrasound are purely intravascular [7]. Regardless of when the liver and liver lesions are visualised, the microbubble signal is a reflection of the relative volume of blood within the field of view. Small-molecule contrast agents for CT and MR imaging, in comparison, diffuse through the vascular endothelium into the tumour interstitium. Thus, CEUS with MFI can be a useful imaging tool for depicting vascular morphology.

On the basis of the above considerations, we hypothesised in the current study that the number of imaging features derived from our clinical experience would be related to the vascular morphological changes due to an increase in liver fibrosis. First, this study aimed to demonstrate this hypothesis by use of an observer performance study; second, if it was correct, to assess the diagnostic accuracy for the prediction of fibrosis stage (according to the new Inuyama classification [8]) by use of the imaging features on MFI of CEUS, which were provided by physicians.

## Materials and methods

This study was approved by the research ethics boards of our institutions; informed consent was obtained from each patient for the use of US data for research purposes, and from each observer for participating in the observer performance study.

### Patients

Between December 2007 and December 2008, we included 60 consecutive patients in this study who had undergone liver biopsy in our institution. A flow diagram of the patients included in this study is shown in Fig. 1.

Patients had a liver biopsy either because they were scheduled for introduction of interferon therapy in our institution and needed assessment of the liver fibrosis stage before treatment ($n$=49), or they were suspected of having chronic liver disease ($n$=11). All CEUS with MFI were performed just before liver biopsy.

After study inclusion, three patients were removed from the investigation because of insufficient liver enhancement (defined as no or only slight enhancement of the liver) due to severe fatty liver, and six were removed because their liver biopsy findings were not suitable for fibrosis staging. Thus, the study group comprised 51 patients. The most common causes of liver disease were hepatitis C virus infection, unclassified, and hepatitis B virus infection (Table 1).

### Clinical reference standard and control subjects

Between December 2007 and December 2008, 11 consecutive patients who were all followed as having liver haemangioma, and met the following criteria, were also included as control subjects (i.e. they had normal livers): CEUS with MFI was performed during the study period for indications other than hepatocellular carcinoma surveillance or assessment of diffuse liver disease (e.g. non-alcoholic fatty liver disease; non-alcoholic steatohepatitis). Informed signed consent was obtained from all patients; there was no documentation of active or past liver disease; there were no risk factors for liver disease (i.e. consumption of two or more alcoholic drinks daily, viral hepatitis

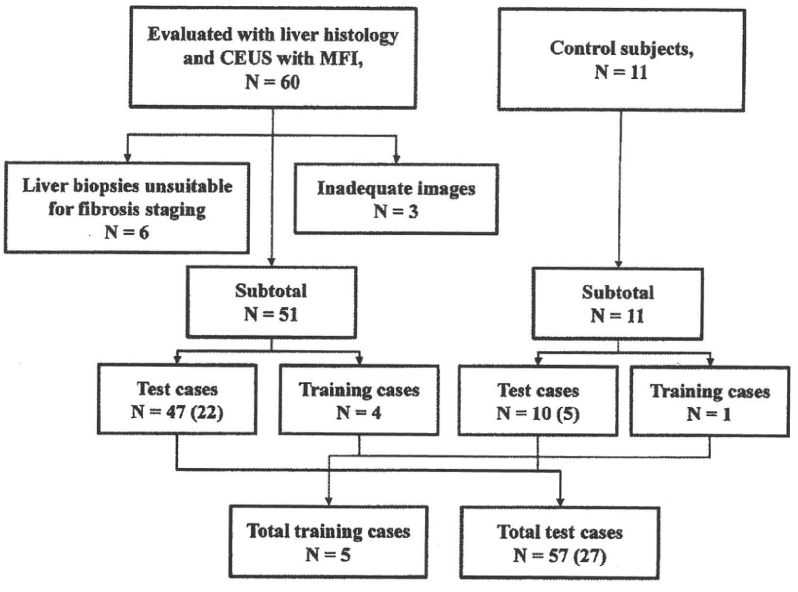


**Fig. 1** Flow diagram of patients who underwent liver biopsy and control subjects during the 12-month study period. The *numbers in parentheses* represent the numbers of cases for which MFIs were obtained twice on the same day by the same operator

**Table 1** Causes of liver disease

| Cause | No. of patients |
|---|---|
| Hepatitis C virus | 36 (70.6%) |
| Hepatitis B virus | 4 (7.8%) |
| Alcohol intake | 2 (3.9%) |
| Alcohol intake, hepatitis B virus | 1 (2.0%) |
| Autoimmune hepatitis | 2 (3.9%) |
| Hepatitis C virus, autoimmune hepatitis | 1 (2.0%) |
| Unclassified | 5 (9.8%) |
| Total | 51 (100%) |

Numbers are based on 51 patients in our study with histopathological analysis as the reference standard

and/or drug abuse); liver function test results obtained within 1 month of the CEUS examination were normal; and viral serology test results were negative.

### Training cases for the observer study and second bolus injection cases for CEUS with MFI examination

To train observers to become familiar with the categorization of images, five of the 62 cases (four biopsy cases and one control subject) were selected based on the following criterion, namely, the cases were the most illustrative of the three imaging features on MFI (Figs. 1, 2, 3, 4). Thus, we enrolled 57 patients: 47 biopsy cases (35 men, 12 women; mean age, 64.2±14.3 years) and 10 control subjects (five men, five women; mean age, 42.2± 10.8 years) in this study.

In order to assess the reproducibility of CEUS with MFI images, we used two CEUS examinations which were performed on the same patients for 22 of the 51 patients and 5 of the 11 control subjects (total 27 cases). These two examinations were performed on the same day on the same patients by the same operator, but from different right intercostal spaces. Finally, we included 84 (57 patients and 27 second bolus injection cases) different cine loops in this observer study.

### US examination technique

Micro-flow imaging is a novel image-processing technique that is accompanied by high mechanical index (MI >1.0) disruptive flash frames and the MIP technique [4, 5]. The MIP processing is initiated after an ultrasound flash frame disrupts bubbles in the field of view. MFI was performed by an experienced hepatologist who was aware of the patients' clinical histories, but was blinded to the other imaging findings and laboratory data.

The contrast agent we used was DD723/NC100100 (Sonazoid; Daiichi Sankyo, Tokyo, Japan), which consists of perflubutane-based microbubbles surrounded by phospholipids with a median diameter of 2–3 μm. The agent was injected as a 0.5-ml bolus into an antecubital vein with a 21-gauge peripheral intravenous cannula, followed by injection of 10 ml saline solution at a rate of 1.0 ml/s. The US equipment used was an SSA-790A (AplioXG; Toshiba, Otawara, Japan) with a 3.75-MHz convex transducer (PVT-375BT). The imaging mode was wideband harmonic imaging (commercially called pulse subtraction) with transmission and reception frequencies of 3.75 and 7.5 MHz, respectively.

The examination was performed on the right lobe of the liver through the intercostal space in all patients at a site as close as possible to a liver biopsy spot, because liver fibrosis is not homogenous over the organ. Before the examination, all of the patients underwent an overnight fast. The detailed US settings were as follows: depth, 5 cm beneath the surface of the skin; focus position, 4 cm beneath the surface of the skin; frame rate, 15 frames per

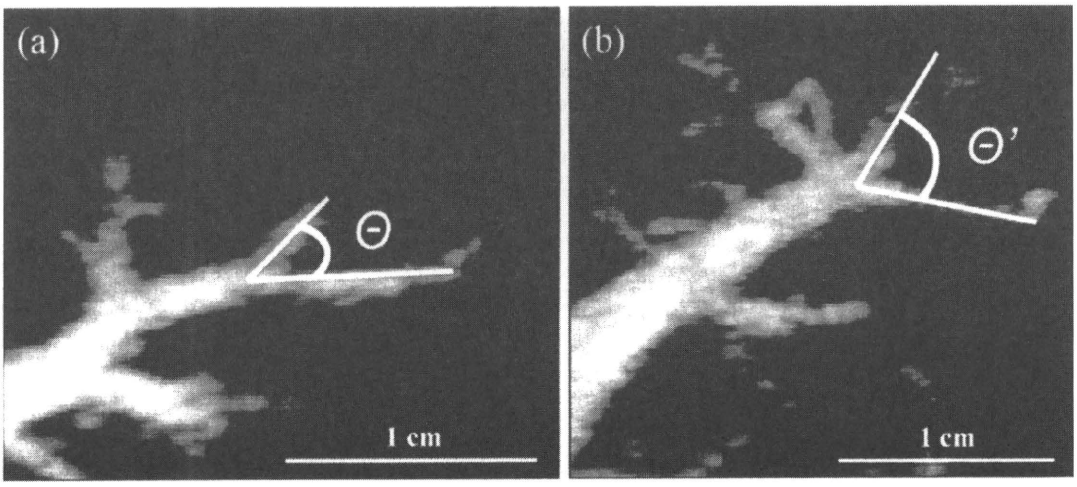


**Fig. 2** These contrast-enhanced US images with micro-flow imaging (MFI) show the sign of angle widening of portal vein branching. The angle of the portal veins with F2 disease (**b**) is wider than that of the portal veins with normal liver (**a**)

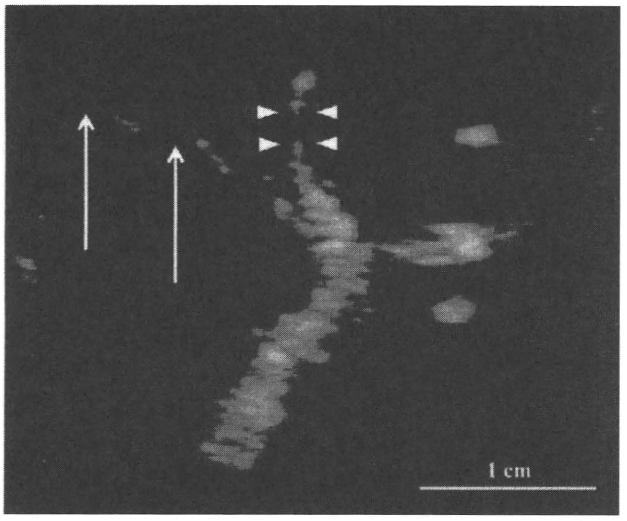


**Fig. 3** This contrast-enhanced US image with micro-flow imaging (MFI) shows signs of the tapering (*arrowheads*) and tortuosity (*arrows*) of portal vein branches

second; and dynamic range, 35 dB. Note that we used the same US settings especially when we performed a second bolus examination. We selected a low MI (<0.20) to avoid the disruption of microbubbles. High MI disruptive flash frames were triggered manually at the peak of parenchymal enhancement, and MFI was initiated with a fixed transducer position. Patients were instructed to hold their breath during MFI (10–12 s) to lessen the effects of tissue motion that results in blurring. Image acquisition was performed during 20 s after high MI disruptive flash frames. The cine loops were recorded on the hard disk of the ultrasound imaging system and were used for off-site analysis.

### Histopathological analysis

In each of 47 patients, liver biopsy specimens were obtained from the anterior segment of the right lobe, with US guidance, by use of an 18-gauge needle (TruCore®; Angiotech, FL, USA). All biopsy specimens were analysed by an experienced pathologist who was blinded to the US results and the biological and clinical data. The new Inuyama scoring system for chronic hepatitis was proposed by the Japanese Liver Study Group in 1994 [8]; it is similar to the classification of chronic hepatitis determined by Desmet et al. [9] and Ludwing [10].

We used the new Inuyama scoring system to assess the fibrosis stage as follows: score 0, no fibrosis; score 1, fibrous portal expansion; score 2, bridging fibrosis; score 3, bridging fibrosis with lobular degeneration; and score 4, cirrhosis. The liver biopsy specimens had to contain at least 10 portal tracts or obvious regenerating nodules to be included in the analysis.

### Image characteristics

We derived three imaging features that could be related to the vascular morphological changes due to the increase in liver fibrosis:

A Angle widening of portal vein branching
B Tapering and interruption of portal vein branches
C Tortuosity and meandering of the portal vein branches

Some examples of imaging features that are related to alterations of portal vein morphology are shown in Figs. 2, 3, 4.

### Observer study

The MFI cine loops were interpreted independently by seven physicians with 7, 10, 20, 10, 9, 6 and 15 years' experience with liver US imaging. Each physician had at least 5 years' experience with CEUS of the liver. Each physician was blinded to the biopsy results, clinical information and other radiological findings. Each physician was asked to rate a confidence level for each imaging feature by using a continuous rating scale displayed on the monitor [11]. This method allowed observing physicians to mark freely any point on the scale based on their own criteria.

All images were interpreted by use of a colour LCD monitor (Flex scan S1961-S; EIZO, Ishikawa, Japan). In order to maintain the observers' attention and avoid their fatigue during the reading session, we divided the 84 cases into three sets (28 cases×3 sets), so that one session would not take longer than 60 min.

In this study, no definitive written criteria for the three imaging features (i.e. angle widening; tapering/interruption; and tortuosity) were given to interpreting physicians

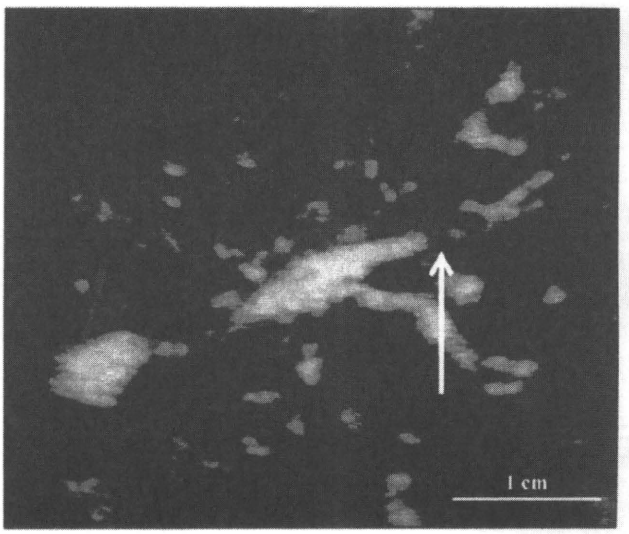


**Fig. 4** This contrast-enhanced US image with micro-flow imaging (MFI) shows a sign of the interruption of portal vein branches (*arrow*)

at the observer study. We, instead, presented five training cases to interpreting physicians before the observer study in an attempt to standardise the physicians' criteria for subjective judgement.

### Statistical analyses

Pearson's correlation coefficients were used for assessment of the correlation between the rating of the confidence level for each imaging feature of MFI and the new Inuyama score as well as a group of normal subjects. The diagnostic performance of each imaging feature of MFI for the distinction between two groups divided by the new Inuyama score was assessed by receiver operating characteristic (ROC) analysis. In this ROC analysis, the average rating of a confidence level for each case among all readers was used as input data for estimating an ROC curve for each imaging feature. The areas under the ROC curves (AUCs) and the 95% confidence intervals (CIs) were calculated by use of a maximum-likelihood estimation program (ROCKIT 0.9B; Charles E. Metz, University of Chicago, Chicago, IL). Finally, sensitivity, specificity and positive and negative predictive values were computed with exact 95% CIs.

Two types of intraclass correlation coefficients, ICC (2,1) and ICC(2,7) [12], were used for assessment of inter-reader reliability among the seven observers for each imaging feature. Here, ICC(2,1) meant the intraclass correlation among the ratings of which the raters were deemed as a random effect, and the unit of analysis was the individual rating. On the other hand, ICC(2,7) meant the intraclass correlation among the ratings of which the raters were deemed as a random effect, but the unit of analysis was the average rating among the seven raters.

Pearson's correlation coefficients were also used for assessment of the reproducibility of MFI images for each imaging feature, with use of the average ratings obtained from the same case groups, but from different imaging planes.

Intraclass correlation coefficients and Pearson's correlation coefficient values of 0.00–0.20 indicated poor agreement; 0.21–0.40, fair agreement; 0.41–0.60, moderate agreement; 0.61–0.80, good agreement; and 0.81–1.00, excellent agreement. All statistical analyses except the ROC curve calculation were performed by use of a computer software package (SPSS 11.0; SPSS, Tokyo, Japan).

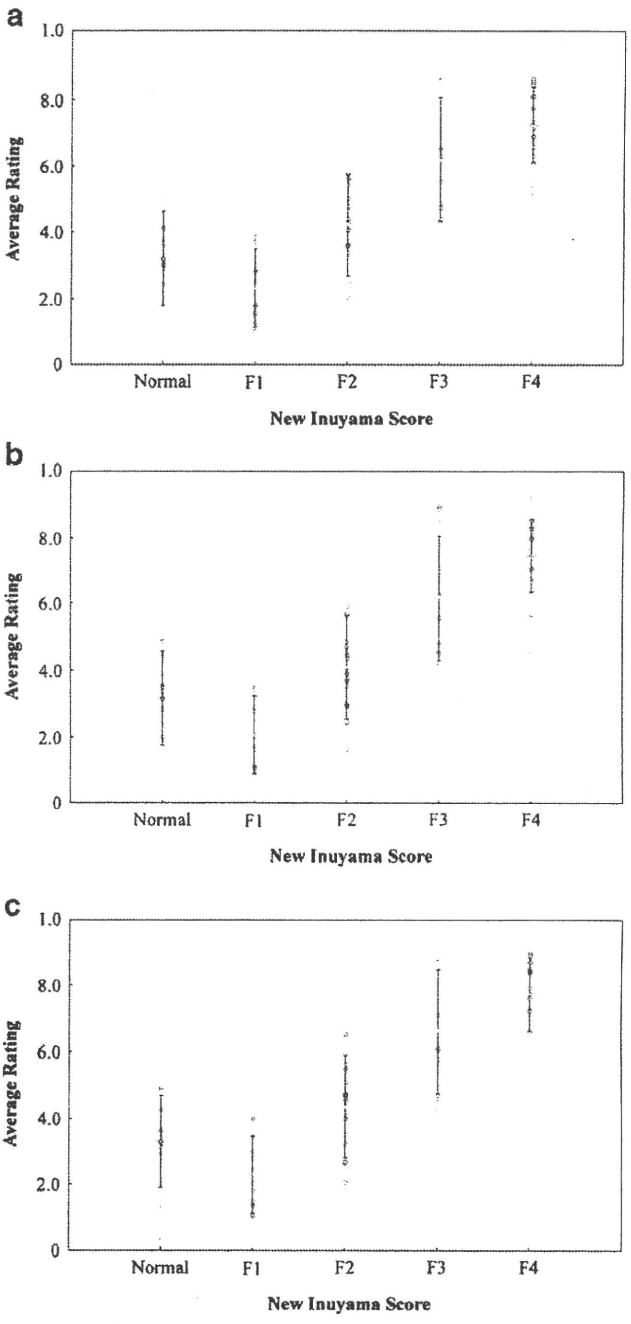


**Fig. 5** Scatter diagrams of **a** imaging feature A (angle widening of portal vein branching), **b** imaging feature B (tapering and interruption of portal vein branches), **c** imaging feature C (tortuosity and meandering of portal vein branches), and for each new Inuyama fibrosis stage. *Line between the error bars* shows the average, and the *error bars* indicate standard deviation. Each plot shows the average rating score among the seven observers

## Results

### Fibrosis staging

None of the 47 patients had a new Inuyama score of F0; 9 (19.1%), a score of F1; 15 (31.9%), a score of F2; 9 (19.1%), a score of F3; and 14 (29.8%), a score of F4. In order to evaluate the relationship between imaging features described by the MFI and the new Inuyama scores, we regarded the cases in the control group as

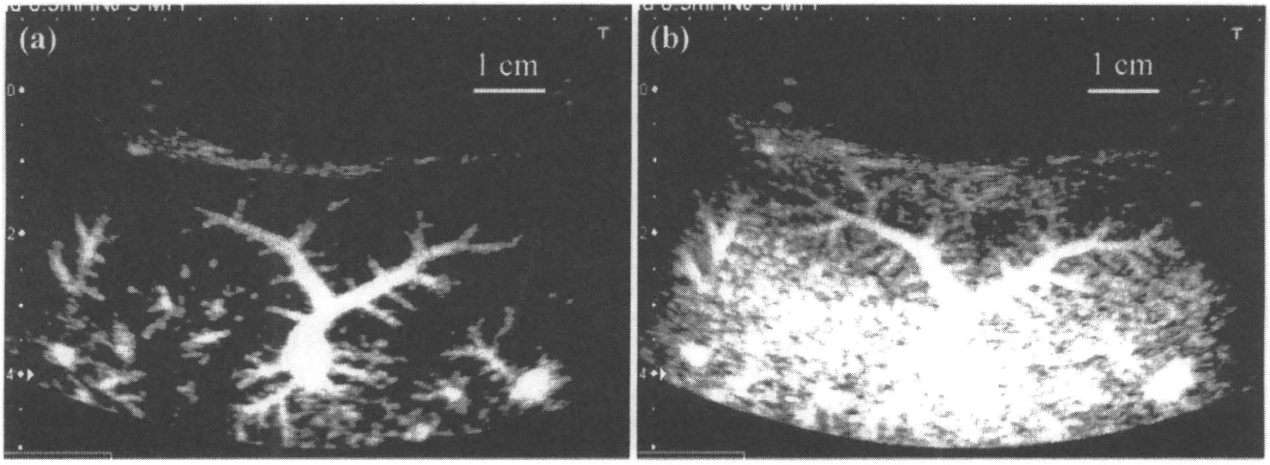


**Fig. 6** Contrast-enhanced US images with micro-flow imaging (MFI) in a 39-year-old healthy man. See also cine loop S1 in the "Electronic supplementary data". **a** MFI image obtained 1 s after the flash shows regularly and continuously branching portal veins. **b** MFI image obtained 6 s after the flash shows spatial homogeneity enhancement of the liver

normal. The second bolus injection cases were as follows: normal; 4 (14.8%) of the 27 patients, F1; 4 (14.8%), F2; 7 (25.9%), F3; 2 (7.4%), F4; 10 (37.0%). As shown in Fig. 5, the confidence level for each imaging feature of MFI increased according to the increase in the liver fibrosis stage, and the correlation with each imaging feature of MFI and the histopathological liver fibrosis stage was relatively high: imaging feature A (angle widening of portal vein branching; $r$=0.794, $p$<0.001), imaging feature B (tapering and interruption of portal vein branches; $r$=0.784, $p$<0.001), and imaging feature C (tortuosity and meandering of portal vein branches; $r$= 0.806, $p$<0.001) correlated with fibrosis stage. Figures 6, 7 and 8 (see also cine loops S1, S2, S3 in the "Electronic supplementary data") show that the degrees of angle widening; tapering/interruption; and tortuosity of the portal veins increased with increasing stage of liver fibrosis.

## ROC analysis

For each new Inuyama fibrosis score threshold without normal (i.e. F1 vs. F2–4, F1–2 vs. F3–4, F1–3 vs. F4), the AUC for each imaging feature of MFI is shown in Table 2. The most discriminating AUC value was 0.964 for F1 vs. F2–4 by use of imaging feature B, 0.968 for F1, 2 vs. F3, 4 by use of imaging feature C, and 0.910 for F1–3 vs. F4 by use of imaging feature A.

Sensitivities, specificities and positive and negative predictive values based on the optimised cut-off value are shown in Table 3.

## Interobserver agreement among seven observers

The results of the interobserver agreement analysis among the seven raters of the MFI images are shown in Table 4.

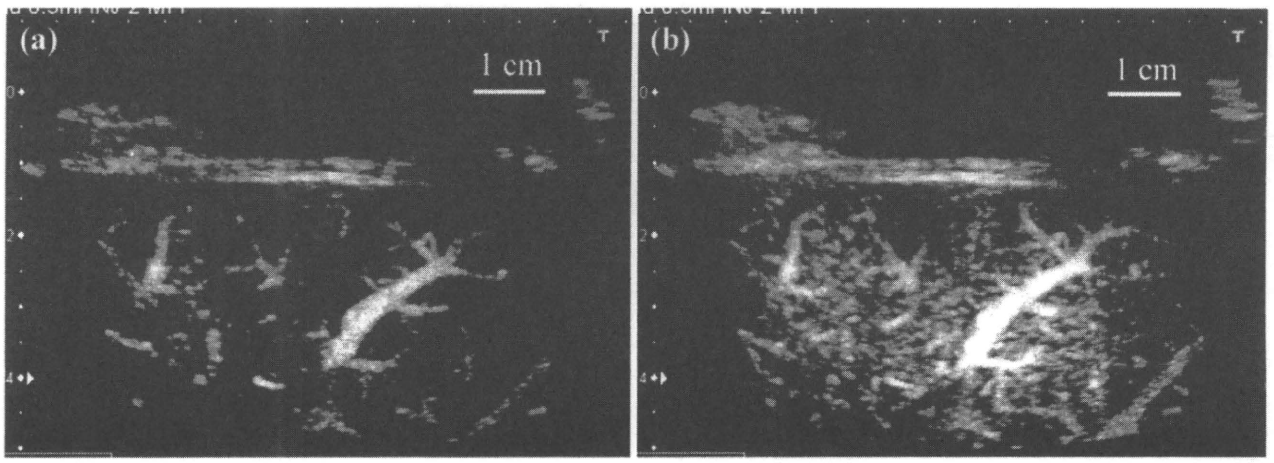


**Fig. 7** Contrast-enhanced US images with MFI in a 68-year-old woman with F2 disease. See also cine loop S2 in the "Electronic supplementary data". **a** MFI image obtained 2 s after the flash shows slight tortuosity and meandering of the portal vein branches compared with Fig. 6a. **b** MFI image 6 s after the flash shows slight spatial heterogeneity of the liver parenchymal enhancement compared with Fig. 6b

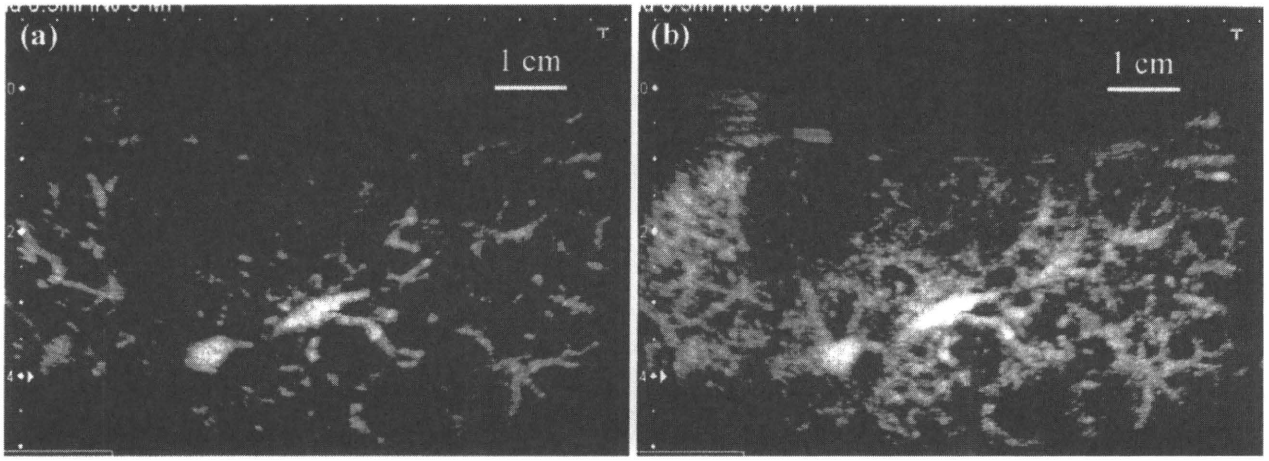


**Fig. 8** Contrast-enhanced US images with MFI in a 65-year-old woman with F4 disease. See also cine loop S3 in the "Electronic supplementary data". **a** MFI image obtained 2 s after the flash shows chaotic vascular changes. **b** MFI image 6 s after the flash shows severe spatial heterogeneity of the liver parenchymal enhancement compared with Figs. 6b and 7b

**Table 2** Average AUC values of each imaging feature of MFI according to the new Inuyama score

| Imaging feature | F1 vs. F2–F4 | F1, F2 vs. F3, F4 | F1–F3 vs. F4 |
|---|---|---|---|
| A | 0.951 (0.859, 0.987) | 0.955 (0.890, 0.985) | 0.910 (0.820, 0.962) |
| B | 0.964 (0.899, 0.990) | 0.950 (0.881, 0.982) | 0.905 (0.814, 0.958) |
| C | 0.952 (0.845, 0.990) | 0.968 (0.913, 0.991) | 0.905 (0.811, 0.960) |

Numbers in parentheses are 95% confidence intervals

*A* angle widening of portal vein branching, *B* tapering and interruption of portal vein branches, *C* tortuosity and meandering of portal vein branches

**Table 3** Diagnostic accuracy of MFI with optimised cut-off values

| | F1 vs. F2–F4 | F1, F2 vs. F3, F4 | F1–F3 vs. F4 |
|---|---|---|---|
| Sensitivity (%) | 87.7 (82.8, 89.2) | 91.4 (82.5, 96.0) | 95.8 (83.1, 99.2) |
| Specificity (%) | 92.3 (70.9, 98.6) | 91.4 (82.5, 96.0) | 80.4 (73.8, 82.2) |
| Positive predictive value (%) | 98.0 (92.6, 99.6) | 91.4 (82.5, 96.0) | 71.9 (62.3, 74.4) |
| Negative predictive value (%) | 63.2 (48.5, 67.5) | 91.4 (82.5, 96.0) | 97.4 (89.3 99.5) |

Numbers in parentheses are 95% confidence intervals

**Table 4** Inter-reader agreement in confidence ratings among the seven observers for each imaging feature

| Imaging feature | A | B | C |
|---|---|---|---|
| ICC(2,1) | 0.560 (0.472, 0.862) | 0.641 (0.530, 0.698) | 0.578 (0.483, 0.672) |
| ICC(2,7) | 0.899 (0.887, 0.942) | 0.917 (0.862, 0.929) | 0.873 (0.824, 0.911) |

Numbers in parentheses are 95% confidence intervals. Agreement was graded as poor (ICC <0.20), moderate (ICC 0.20 to <0.40), fair (0.40 to <0.60), good (0.60 to <0.80), or very good (0.80–1.00)

*ICC* intraclass correlation coefficients, *A* angle widening of portal vein branching, *B* tapering and interruption of portal vein branches, *C* tortuosity and meandering of portal vein branches

ICC(2,1) (i.e. the unit of analysis was the individual rating) showed relatively low interobserver agreement (0.560–0.641). Conversely, ICC(2,7) (i.e. the unit of analysis was the average rating among the seven raters) showed high values (0.873–0.917), which indicated the reliability of the MFI examination when the average rating score of the seven observers was high.

Reproducibility of MFI images

For each MFI feature, the correlation coefficients of the average rating scores between different images from the same cases were 0.831 for A; 0.828 for B and 0.854 for C (mean, 0.838±0.01 [standard deviation]), which indicated the high reproducibility of MFI images.

## Discussion

The results of our study demonstrated that the image characteristics described on the MFI showed good correlation with the degree of liver fibrosis, and thus, the MFI of CEUS may be useful for non-invasive staging fibrosis. In our study, CEUS with MFI enabled us to clearly separate the intermediate fibrosis stages (i.e. F1 vs. F2–4). With an optimised cut-off value for F1 vs. F2–4, the sensitivity was 87.7% at a specificity of 92.3%. This high accuracy is clinically important because, according to the American Association for the Study of Liver Diseases, patients with hepatitis C genotype 1 infection should be treated only when substantial fibrosis (F≥F2) is observed [13].

In our study, advanced fibrosis and cirrhosis were also diagnosed accurately (i.e. F1–2 vs. F3–4). With an optimised cut-off point for F1–2 vs. F3–4, a sensitivity of 91.4% was at a specificity of 91.4%. This high accuracy in the diagnosis of advanced fibrosis is also important because patients with advanced fibrosis should be screened for portal hypertension and hepatocellular carcinoma [14, 15].

Our results also showed that, as the degree of liver fibrosis increased, the rating score of each imaging feature on MFI (e.g. angle widening, tapering/interruption and tortuosity) tended to be high in a stepwise fashion. Kelty et al. [16] reported that intrahepatic vascular morphological changes within the cirrhotic liver were caused mainly by the pressure of growth and expansion of the regenerative nodule against the rather rigid connective tissue surroundings. The results of our study, however, suggest that those vascular disorders might already have existed in the intermediate and advanced fibrosis stages.

We investigated the relationship between intrahepatic vascular morphological changes and pathological liver fibrosis stage in the study. However, as we described in the figure captions (Figs. 6, 7, 8), heterogeneity of the liver parenchymal enhancement tended to be observed according to the increase in the liver fibrosis stage, and it could be also one of the important image features. Thus, it would affect the results of our study.

The development of non-invasive biomarkers of liver fibrosis would reduce biopsy-related risk and costs and thus facilitate earlier diagnosis and improved monitoring of the progression of chronic liver disease. A number of serological markers of liver fibrosis have been developed in chronic viral hepatitis. The techniques include simple tests such as the aspirate transaminase-to-platelet ratio index (APRI) [17], platelet count, the prothrombin index, and more complex tests, such as the FibroTest (Biopredictive, Paris, France) [18], which were based on a combination of basic serum markers. However, previous reports [19, 20] showed that these serum scoring systems provided accurate differentiation of only two stages of the fibrosis spectrum (i.e. minimal and advanced fibrosis). Thus, these scoring systems are less effective for differentiating the intermediate stages of fibrosis. Moreover, the main weakness of these tests is that some parameters can be influenced by extrahepatic diseases.

Several liver imaging methods have also been used for the diagnosis and staging of liver fibrosis. Most of these methods, including conventional US, transient US elastography, double-contrast material-enhanced MR imaging, perfusion MR imaging and diffusion MR imaging, are limited to the detection of advanced fibrosis [21–25]. The effectiveness of these methods in the detection of significant fibrosis (F≥F2) remains to be seen. MR elastography, however, may potentially enable significant fibrosis (F≥F2) to be diagnosed [26].

Our study had several limitations. First, because we are reporting our initial experience, the results were limited by a small sample size, and the study population of each category was also imbalanced. In particular, there were no patients with histopathologically proven F0. Although we regarded a control group as normals, there might have been contamination of liver fibrosis changes among the cases in the control group. Second, there were large overlaps in the ratings of each imaging feature among the different levels of fibrosis, and this may limit the clinical applicability of this study. Third, we eliminated patients who had severe steatosis from our study subjects. In patients with severe steatosis, it is difficult to obtain good-quality images because of its deep attenuation, especially when we use low MI harmonic imaging. Fourth, our results were based on subjective ratings of seven physicians. It is therefore unavoidable that inter- and intra-observer agreements are relatively low. We will develop a computer-aided diagnosis (CAD) scheme designed to discriminate among liver fibrosis stages in future work. Fifth, histopathological findings can be an imperfect reference standard. It is known that the fibrosis scores of biopsy specimens may cause underestimations of the severity of fibrosis [27–29]. Sixth, whilst the ROC-generated sensitivity and specificity are acceptably good, the potential problem is in standardizing the categories of vascular changes used in this study. In this study, no definitive written criteria for the rating of the imaging features were provided to interpreting physicians in the

observer study. Instead, we tried to have interpreting physicians acquire common criteria for their judgement by training them with the use of five instructive cases before the observer study, which might have given rise to greater inter- and intraobserving physician variations. However, there was indeed a possibility that definite criteria, if established, might have minimised the influence of physicians' subjectivity, but the interpretation process might have been more complicated. Moreover, it is unclear at the moment how detailed the criteria for the rating of the imaging features should be. We consider it an important future issue to define the criteria precisely.

In conclusion, our preliminary findings suggest that assessment of morphological intrahepatic vascular changes on MFI can be used for quantifying liver fibrosis. MFI can easily be incorporated into a routine CEUS protocol. It may be possible to use MFI findings to determine the indication for antiviral treatment and for follow-up of patients with chronic liver disease.

**Acknowledgments** The authors are grateful to Tomihiko Hirokawa, MD, Liu Guang-Jian, MD, Yasuharu Imai, MD, Junich Taira, MD, and Takatomo Sano, MD, for participating as observers; and to Mrs. Elisabeth Lanzl for improving the manuscript.

## References

1. Anthony PP, Ishak KG, Nayak NC et al (1978) The morphology of cirrhosis. Recommendations on definition, nomenclature, and classification by a working group sponsored by the World Health Organization. J Clin Pathol 31:395–414
2. Daniel PM, Prichard MML, Reynell PC (1952) The portal circulation in experimental cirrhosis of the liver. J Pathol Bacteriol 114:53–60
3. Popper H, Elias H, Patty DE (1952) Vascular pattern of the cirrhotic liver. Am J Clin Pathol 22:717–729
4. Sugimoto K, Moriyasu F, Kamiyama N et al (2008) Analysis of morphological vascular changes of hepatocellular carcinoma by micro flow imaging using contrast-enhanced sonography. Hepatol Res 38:790–799
5. Shiraishi J, Sugimoto K, Moriyasu F, Kamiyama N, Doi K (2008) Computer-aided diagnosis for the classification of focal liver lesions by use of contrast-enhanced ultrasonography. Med Phys 35:1734–1746
6. Wilson SR, Jang HJ, Kim TK, Iijima H, Kamiyama N, Burns PN (2008) Real-time temporal maximum-intensity projection imaging of hepatic lesions with contrast-enhanced sonography. AJR Am J Roentgenol 190:691–695
7. Burns PN (2002) Contrast ultrasound technology. In: Solbital L, Martegani A, Leen E, Correas JM, Burns PN, Becker D (eds) Contrast-enhanced ultrasound of liver diseases. Springer, Milan, pp 1–19
8. Ichida F, Tsuji T, Omata M et al (1996) New Inuyama classification: new criteria for histological assessment of chronic hepatitis. Int Hepatol Commun 6:112–119
9. Desmet VJ, Gerber M, Hoofnagle JH, Manns M, Scheuer PJ (1994) Classification of chronic hepatitis: diagnosis, grading and staining. Hepatology 19:1513–1520
10. Ludwing J (1993) The nomenclature of chronic active hepatitis; An obituary. Gastroenterology 105:274
11. MacMahon H, Engelman R, Behlen FM et al (1999) Computer-aided diagnosis of pulmonary nodules: results of a large-scale observer test. Radiology 213:723
12. Shrout PE, Fleiss JL (1979) Intraclass correlations: uses in assessing rater reliability. Psychol Bull 86:420–428
13. Strader DB, Wright T, Thomas DL, Seeff LB (2004) Diagnosis, management, and treatment of hepatitis C. Hepatology 39:1147–1171
14. Bruix J, Sherman M (2005) Management of hepatocellular carcinoma. Hepatology 42:1208–1236
15. De Franchis R (2005) Evolving consensus in portal hypertension: report of the Baveno IV Consensus Workshop on Methodology of Diagnosis and Therapy in Portal Hypertension. J Hepatol 43:167–176
16. Kelty RH, Baggenstoss AH, Butt HR (1950) The relation of the regenerated liver nodule to the vascular bed in cirrhosis. Gastroenterology 15:285–295
17. Wai CT, Greenson JK, Fontana RJ et al (2003) A simple noninvasive index can predict both significant fibrosis and cirrhosis in patients with hepatitis C. Hepatology 38:518–526
18. Imbert-Bismut F, Ratziu V, Pieroni L, Charlotte F, Benhamou Y, Poynard T (2001) Biochemical markers of liver fibrosis in patients with hepatitis C virus infection: a prospective study. Lancet 357:1069–1075
19. Rocky DC, Bissel DM (2006) Noninvasive measures of liver fibrosis. Hepatology 43:S113–S120
20. Bataller R, Brenner DA (2005) Liver fibrosis. J Clin Invest 115:209–218
21. Colli A, Fraquelli M, Andreoletti M, Marino B, Zuccoli E, Conte D (2003) Severe liver fibrosis or cirrhosis: accuracy of US for detection - analysis of 300 cases. Radiology 227:89–94
22. Fridrich-Rust M, Ong MF, Herrmann E et al (2007) Real-time elastography for noninvasive assessment of liver fibrosis in chronic viral hepatitis. AJR Am J Roentgenol 188:758–764
23. Aguirre DA, Behling CA, Alpert E, Hassanein TI, Sirlin CB (2006) Liver fibrosis: noninvasive diagnosis with double contrast material-enhanced MR imaging. Radiology 239:425–437
24. Annet L, Materne R, Danse E, Jamart J, Horsmans Y, Van Beers BE (2003) Hepatic flow parameters measured with MR imaging and Doppler US: correlation with degree of cirrhosis and portal hypertension. Radiology 229:409–414
25. Koinuma M, Ohashi I, Hanafusa K, Shibuya H (2005) Apparent diffusion coefficient measurements with diffusion-weighted magnetic resonance imaging for evaluation of hepatic fibrosis. J Magn Reson Imaging 22:80–85
26. Huwart L, Sempoux C, Salameh N et al (2007) Liver fibrosis: noninvasive assessment with MR elastography versus aspirate aminotransferase-to-platelet ratio index. Radiology 245:458–466
27. Poniachik J, Bernstein DE, Reddy KR et al (1996) The role of laparoscopy in the diagnosis of cirrhosis. Gastrointest Endosc 43:568–571
28. Pagliaro L, Rinaldi F, Craxi A et al (1983) Percutaneous blind biopsy versus laparoscopy with guided biopsy in diagnosis of cirrhosis: a prospective, randomized trial. Dig Dis Sci 28:39–43
29. Maharaj B, Maharaj RJ, Leary WP et al (1986) Sampling variability and its influence on the diagnostic yield of percutaneous needle biopsy of the liver. Lancet 1:523–525

doi:10.1111/j.1440-1746.2008.05549.x

GASTROENTEROLOGY

# Long-term results of balloon-occluded retrograde transvenous obliteration for gastric variceal bleeding and risky gastric varices: A 10-year experience

Tomohiko Akahoshi,* Makoto Hashizume,† Morimasa Tomikawa,* Hirofumi Kawanaka,* Shohei Yamaguchi,† Kouzo Konishi,* Nao Kinjo* and Yoshihiko Maehara*

Departments of *Surgery and Science and †Disaster and Emergency Medicine, Graduate School of Medical Sciences, Kyushu University, Fukuoka, Japan

**Key words**
balloon-occluded retrograde transvenous obliteration, esophageal varices, gastric varices, long-term result, portal hypertension.

Accepted for publication 8 May 2008.

**Correspondence**
Dr Tomohiko Akahoshi, Department of Surgery and Science, Graduate School of Medical Sciences, Kyushu University, 3-1-1 Maidashi, Higashi-ku, Fukuoka 812-8582, Japan. Email: a_tom411@yahoo.co.jp

## Abstract

**Background and Aim:** Balloon-occluded retrograde transvenous obliteration (B-RTO) is a new alternative treatment for gastric varices (GVx), but the long-term efficacy is not known. We investigated the long-term effects of B-RTO on rebleeding, prevention of first bleeding, mortality and occurrence of risky esophageal varices (EVx).

**Methods:** B-RTO was performed in 68 cirrhotic patients with GVx. Twenty patients had recent bleeding, transiently treated by endoscopic Histoacryl injection or balloon tamponade. Forty-eight patients had varices likely to bleed, but no bleeding. After B-RTO, the recurrent bleeding, occurrence of EVx and mortality over the long-term were evaluated.

**Results:** B-RTO was successfully performed in 63 of 68 patients (92.6%). Varices eradication was confirmed by endoscopy in 61 of 63 patients (96.6%). During follow up, GVx bleeding occurred in two patients (3.2%). The 8-year cumulative rebleeding rates of patients with bleeding and risky GVx were 14% and 0%, respectively. Risky EVx occurred in 10 patients (17%) and the cumulative occurrence rate was 22% in 8 years. The cumulative occurrence rate of risky EVx was higher in GVx with EVx (GOV2-GVx) compared to GVx without EVx (IGV1, $P < 0.05$). No ectopic variceal bleeding occurred. No patients died from variceal bleeding. Hepatocellular carcinoma was the only significant prognostic factor ($P < 0.05$).

**Conclusion:** B-RTO is beneficial over the long-term, despite worsening EVx in some patients, because of excellent treatment efficacy and improved mortality. We believe that B-RTO can become a first-choice radical treatment following hemostasis for gastric variceal bleeding and prophylactic treatment for risky GVx.

## Introduction

Although the incidence of bleeding from gastric varices (GVx) is relatively low (10–36%), when it does occur, it is massive and increases patient mortality.[1–4] The treatment of esophageal variceal (EVx) bleeding is highly differentiated with several effective treatments available.[5–9] In contrast, bleeding from GVx continues to be a therapeutic challenge. A number of investigators have reported that endoscopic injection sclerotherapy (EIS) is ineffective for the treatment of GVx, particularly isolated GVx.[10,11] GVx generally exist as a part of a gastrorenal shunt or gastroinferior phrenic caval shunt, resulting in outflow into the systemic circulation.[12] Because these anatomical characteristics create a higher blood flow volume through the shunt, causing a rapid escape of sclerosing solution into the systemic circulation during EIS, conventional EIS is not effective for the treatment of GVx.

Advances in non-endoscopic techniques, such as surgical procedures or transjugular intrahepatic portosystemic shunt (TIPS), have had a significant impact on the management of portal hypertension. Most such treatments, however, are not ideal as first-choice therapies for GVx, because of their technical requirements or level of invasiveness.[13,14] Balloon-occluded retrograde transvenous obliteration (B-RTO) was developed and established as a superior effective treatment for fundal GVx and hepatic encephalopathy.[12,15] Two Japanese groups recently demonstrated the long-term effectiveness of B-RTO for the treatment of risky GVx.[16,17] In most of the cases examined, however, the treatment was prophylactic; thus, the long-term efficacy of B-RTO against gastric bleeding has not been demonstrated. More definitive evidence of the long-term effectiveness of B-RTO is required to obtain the acceptance of medical groups in other countries. Therefore, the aim of this study was to evaluate the long-term results of the B-RTO



Journal of Gastroenterology and Hepatology 23 (2008) 1702–1709 

procedure in patients with GVx bleeding or risky GVx and to clarify its role in the treatment of GVx.

## Methods

### Patients

Between August 1994 and August 2004, 912 patients with portal hypertension were admitted to Kyushu University because of variceal bleeding or risky large esophageal or gastric varices. Of 912 patients, 90 (9.8%) were diagnosed with large isolated gastric varices (IGV1) or large gastric varices with esophageal varices (GOV2).[1] In 68 of 90 patients (75.6%), gastrorenal shunts were confirmed by computed tomography and angiography (Fig. 1a), and B-RTO was then performed to treat the GVx.

There were 44 men and 24 women in the study with ages ranging 32–74 years (mean age, 56.6 ± 10.2 years; Table 1). Of the 68 cases, 20 had an endoscopically confirmed episode of GVx bleeding. In 14 patients with active bleeding, hemostasis was achieved by injection sclerotherapy of N-butyl-2-cyanoacrylate (histoacryl, Braum, Melsungen, Germany) or a Sengstaken–Blakemore tube. Six patients had an episode of recent bleeding as evidenced by the presence of GVx with fibrin clots. Of the 68 cases, 48 had no bleeding episodes, but endoscopic examination indicated the presence of risky GVx based on form, location and color, as described previously.[3]

Concomitant esophageal varices were all treated by endoscopic variceal ligation or endoscopic injection sclerotherapy during the same administration period.

### B-RTO

Balloon-occluded retrograde transvenous obliteration was performed according to the method reported by Kanagawa *et al.*[12] A catheter for B-RTO (6.5-Fr; Create Medic, Tokyo, Japan) was introduced into the gastrorenal shunt via the right femoral vein. The gastrorenal shunt was visualized using 10–20 mL iopamidol to judge whether shunt occlusion was achieved and to estimate the amount of sclerosant to be used. If accumulation could not be achieved due to other outflow routes (e.g. cardiac-phrenic vein, umbilical vein), absolute ethanol, 50% glucose and/or coils were used to embolize these small outflow vessels. After confirming the accumulation of iopamidol in the GVx, a 5% solution of ethanolamine oleate with iopamidol (EOI) was injected slowly until there was sufficient accumulation in the GVx (Fig. 1b). Simultaneously, 4000 units of haptaglobin (Yoshitomi, Osaka, Japan) was administered i.v. for protection against renal damage from the ethanolamine oleate sclerosant.[18] The balloon was deflated 24 h after injection of the sclerosant.

### Occurrence of risky EVx after B-RTO

Occurrence of risky EVx was evaluated by endoscopic examination at 3–4-month intervals. Risky EVx was defined by the Japanese portal hypertension guidelines.[19]

Esophageal varices that were moderate or huge in size (F2 or F3) and had one of several marks (red wale marking, cherry red spot or hematocystic spot), were defined as risky EVx, which are likely to bleed.

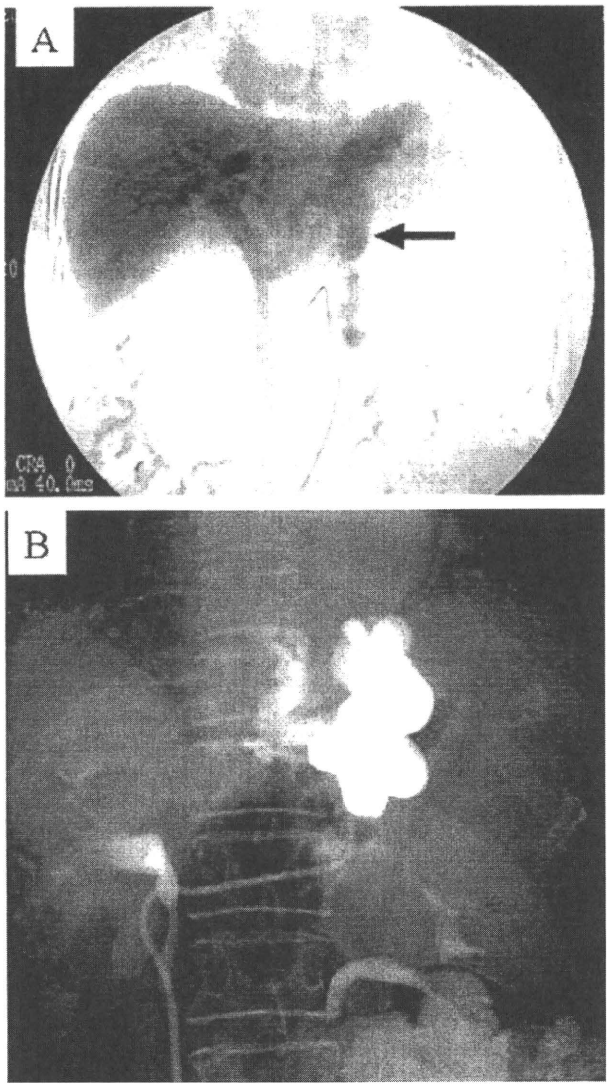


**Figure 1** (a) Superior mesenteric arteriography showing a gastrorenal shunt. Celiac and/or superior mesenteric arteriography can detect the major shunt (arrow), for which the balloon-occluded retrograde transvenous obliteration (B-RTO) procedure is indicated. (b) In most cases, after controlling the other outflow routes, a sufficient accumulation of 5% ethanolamine oleate with iopamidol (EOI) was obtained in the gastric varices.

### Follow up

Complete eradication of the GVx was confirmed 4 weeks later by endoscopic examination (Fig. 2). The average observation period after B-RTO was 66.2 ± 31.6 months (range, 24–127 months) with repeated endoscopic examinations at 3–4-month intervals. Twenty patients (seven patients were bleeding cases from GVx) were followed for more than 96 months (8 years).

**Table 1** Clinical characteristics of patients with gastric varices

| | No. patients |
|---|---|
| No. of patients (men : women) | 68 (44 : 24) |
| Mean age/range (years) | 56.6 ± 10.2 (32–74) |
| Etiology of gastric varices | |
| Cirrhosis | |
| Viral hepatitis (HCV/HBV) | 50 (43/7) |
| Alcoholism | 7 |
| Unknown | 4 |
| Primary biliary cirrhosis | 2 |
| Primary sclerosing cholangitis | 1 |
| Idiopathic portal hypertension | 2 |
| Post-living donor liver transplantation | 2 |
| Child–Pugh classification (A/B/C) | 27/28/13 |
| Association with hepatocellular carcinoma | 24 (35.3%) |
| Association with esophageal varices (GOV2) | 31 (45.6%) |
| Gastric varices with hemorrhage | 20 (29.4%) |
| Form of gastric varices (F1/F2/F3) | 0/3/17 |
| Initial treatment | |
| EIS/S-B tube/spontaneous hemostasis | 10/4/6 |
| GOV2/IGV1 | 10/10 |
| High risk gastric varices | 48 (70.6%) |
| Form of gastric varices (F1/F2/F3) | 0/18/35 |
| GOV2/IGV1 | 21/27 |
| Average follow-up term (months) | 66.2 ± 31.6 |

EIS, endoscopic injection sclerotherapy; GOV2, gastric varices concomitant with esophageal varices; IGV1, gastric varices without esophageal varices; S-B tube, Sengstaken–Blakemore tube.

### Percutaneous transhepatic portography assessment

Percutaneous transhepatic portography (PTP) was performed in 17 of 68 patients (25%) during the B-RTO procedure. Portal venous pressure (PVP) was measured. In addition, the hemodynamic characteristics were assessed. Special concern was taken to determine whether the PVP or inflow route differed between IGV1 and GOV2. Further, the amount of ethanol required to obstruct the collaterals and the occurrence of risky EVx were also compared between IGV1 and GOV2.

### Statistics

Cumulative survival curve, recurrent bleeding-free time curve and risky EVx occurrence curve were calculated according to the Kaplan–Meier method. A log–rank test was used for the comparison between each curve. Data were compared between two groups and tested using the unpaired Student's *t*-test. Qualitative data were analyzed by the Fisher's exact test. $P < 0.05$ was considered to be statistically significant.

## Results

The B-RTO procedure was successfully performed in 63 of 68 patients (92.1%; Table 2). The average time required for the B-RTO procedure was 50.1 ± 18.4 min ($n = 63$). Two patients had large gastrorenal shunts, so the balloon did not sufficiently occlude the shunt. Three cases had several outflow routes that were not occluded, despite using ethanol, 50% glucose and/or coils, resulting in insufficient accumulation of the sclerosant. These patients underwent gastric devascularization and splenectomy (Hassab's operation) or EIS with Histoacryl combined with ethanolamine oleate.

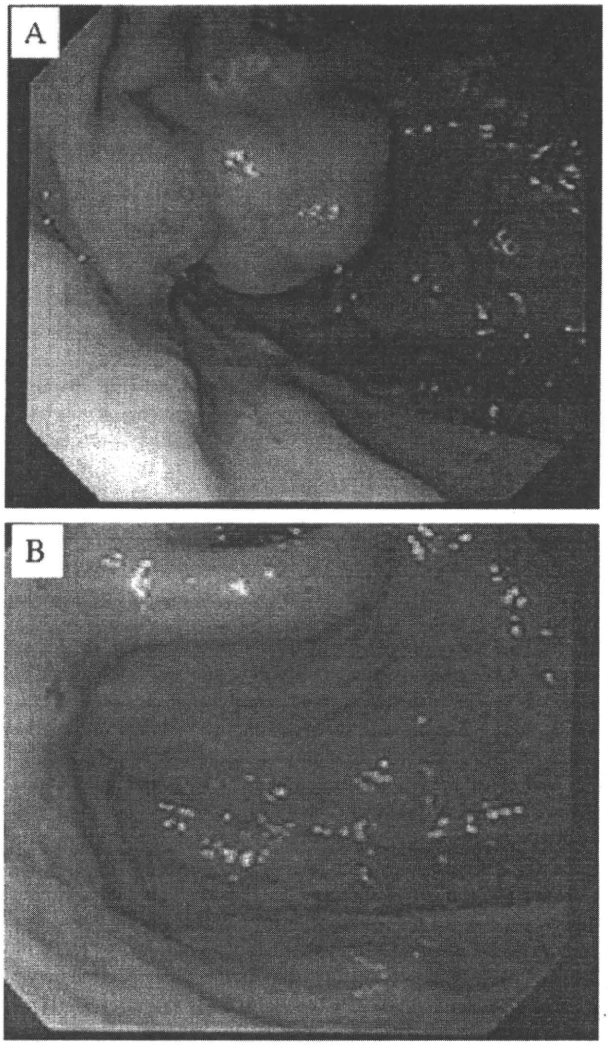


**Figure 2** (a) Endoscopic image showed tumorous (F3) risky gastric varices. (b) Endoscopic image obtained 3 months after balloon-occluded retrograde transvenous obliteration (B-RTO) revealed eradication of gastric varices.

The total eradication rate for GVx was 61/63 (96.8%). The eradication rate was 100% (29/29) in the GOV2 patients and 94.1% (32/34) in the IGV1 patients. The average amount of 5% EOI used was 31.8 ± 16.8 mL. Absolute ethanol was used in 26 patients (average amount, 2.4 ± 1.4 mL) and 50% glucose was used in 13 patients (average amount, 11.4 ± 13.5 mL). Nine patients had both ethanol and 50% glucose to occlude small collateral vessels. Coils were used in five patients for obliteration of outflow collaterals, which were difficult to occlude with ethanol or 50% glucose. Most patients did not require additional treatment,


Journal of Gastroenterology and Hepatology **23** (2008) 1702–1709 

**Table 2** Balloon-occluded retrograde transvenous obliteration results

| | No. patients (%) |
|---|---|
| Success of procedure | 63/68 (92.6) |
| Amount of 5% EOI | 31.8 ± 16.8 mL |
| Obliteration of outflow routs | 26/68 (41.3) |
| Absolute ethanol | 26 (38.2) |
| 50% glucose | 13 (19.1) |
| Coils | 5 (7.3) |
| Eradication rate | 61/63 (96.8) |
| Recurrence rate | 2/63 (3.2) |
| Bleeding rate | 2/63 (3.2) |
| Complication | |
| Major | |
| Pulmonary infarction | 1 (1.6) |
| Ventricular fibrillation | 1 (1.6) |
| Minor | |
| Hematuria | 37 |
| Fever (>37.5°C) | 25 |
| Ascites | 4 |

EOI, ethanolamine oleate with iopamidol.

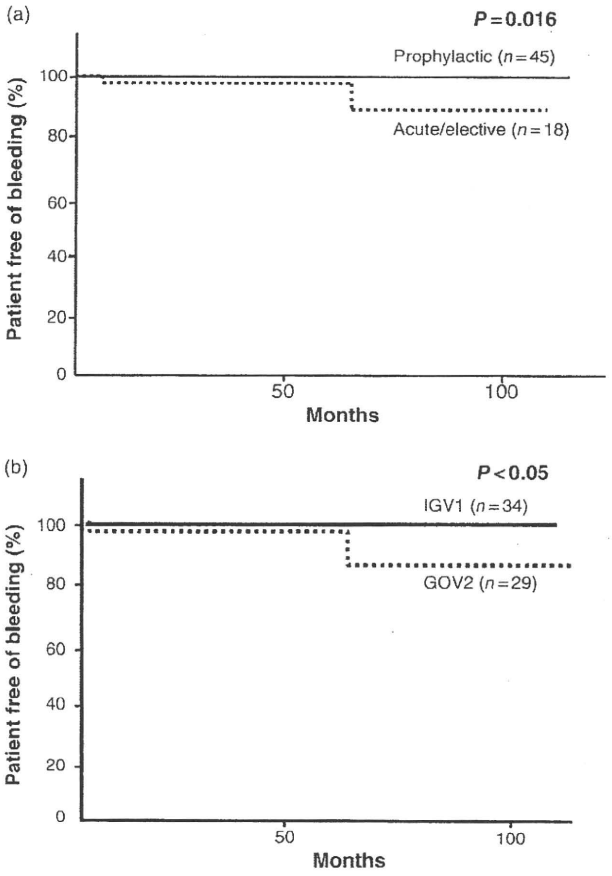


**Figure 3** Cumulative rebleeding-free rate by Kaplan–Meier analysis. (a) Solid line, prophylactic cases (patients with risky gastric varices); dotted line, acute or elective cases (patients with gastric variceal hemorrhage). (b) Solid line, IGV1 cases (patients without esophageal varices [EVx]); dotted line, GOV2 cases (patients with EVx).

but two patients required EIS treatment to eradicate GVx. These two patients were easily treated with EIS using only ethanolamine oleate, because the varices were almost thrombosed by B-RTO.

Recurrent bleeding was observed in two patients during the follow up. Both patients had a previous history of GVx bleeding. One patient had hepatocellular carcinoma (HCC) combined with a portal thrombus 6 years after B-RTO. Recurrent bleeding was controlled by EIS with Histoacryl. The cumulative rebleeding rate of the GVx patients with previous bleeding was 2.4% at 1 year, 2.4% at 5 years and 14.3% at 8 years (Fig. 3a). In patients without previous bleeding, the bleeding rate was 0% during the entire study period (Fig. 4a). On the other hand, no IGV1-GVx bleeding occurred in any patients, but GOV2-GVx bleeding occurred in two patients. The cumulative GOV2-GVx bleeding rate after B-RTO at 1, 5 and 8 years was 3.4%, 3.4% and 17.2%, respectively (Fig. 3b). No patients died after B-RTO due to GVx bleeding during the follow up.

The cumulative survival rate at 3, 5 and 8 years was 96.5%, 81.7% and 79.0%, respectively (Fig. 4a). To date, 11 patients have died: four from liver failure, six from HCC and one due to cerebral infarction. The differences in each survival curve among the three Child–Pugh classes were not significant ($P = 0.952$). There were no significant differences between non-HCC patients of Child–Pugh A ($n = 19$) and of Child–Pugh B or C ($n = 21$) classifications ($P = 0.801$; Fig. 4b). There was a significant difference in the survival curves of the patients with and without HCC ($P = 0.021$; Fig. 4c).

## Complications

Sclerosant-induced pulmonary embolism occurred in one patient. Blood gas analysis revealed severe hypoxemia and a pulmonary perfusion scintigram revealed decreased perfusion in the peripheral area of both lungs. In that patient, 40 mL of 5% EOI exited to the systemic circulation due to the collapse of the balloon obstructing the gastrorenal shunt. Anticoagulant therapy with continuous i.v. administration of heparin was initiated immediately and the clinical condition improved markedly. Ventricular fibrillation, thought to be due to acute hypertension, occurred in one patient. The patient was immediately defibrillated by emergency electric conversion. There were minor complications, such as fever of more than 37.5°C, hematuria and ascites, but these complications did not prolong the hospital stay (Table 2).

## Occurrence of risky esophageal varices

Risky EVx developed in 10 patients, and three of them bled. Of the 10 patients, seven who developed risky EVx after B-RTO had EVx before the B-RTO procedure. Their varices were all small and not indicated for treatment according to the Japanese portal hypertension guidelines. Episodes of EVx worsening or bleeding in five patients were noted within 2 months. The patients with worsening EVx or bleeding EVx were treated with EIS or endoscopic variceal ligation and their varices were all eradicated. Death due to EVx bleeding did not occur. The cumulative occurrence rate of risky

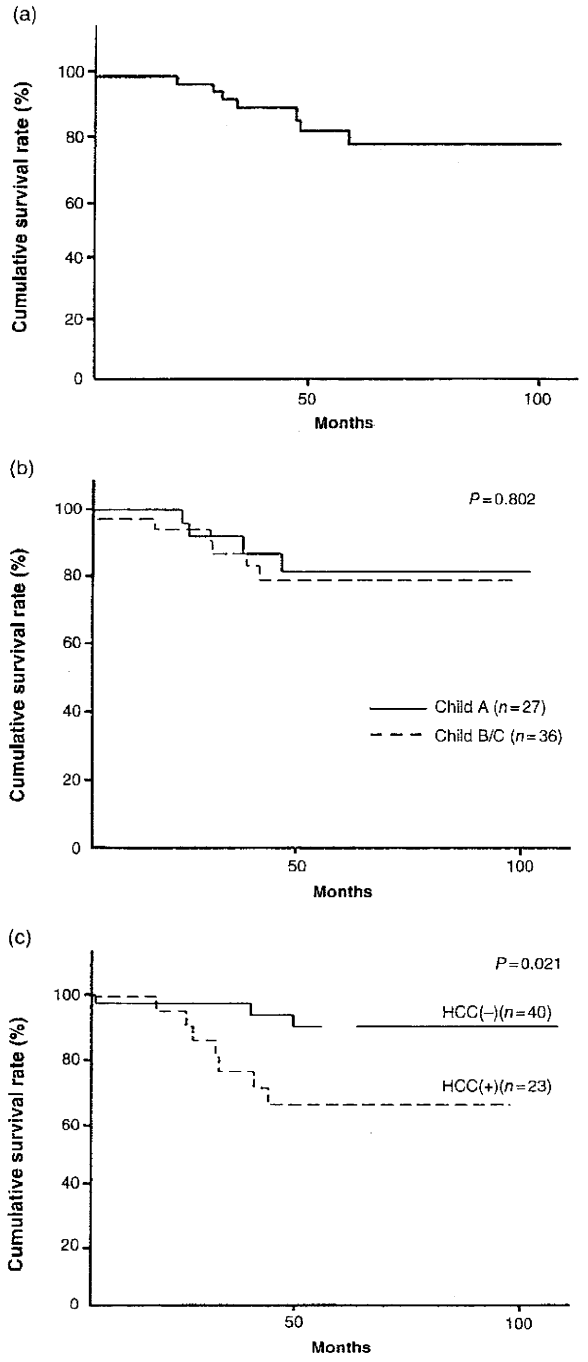


**Figure 4** (a) Cumulative total survival rate after balloon-occluded retrograde transvenous obliteration (B-RTO) (Kaplan–Meier analysis). (b) Cumulative survival rate after B-RTO in relation to the Child–Pugh classification (Kaplan–Meier analysis). The difference between the two groups (non-hepatocellular carcinoma [HCC] patients) was not statistically significant ($P = 0.802$). (c) Cumulative survival rate after B-RTO with or without HCC. The difference between the two groups was statistically significant ($P = 0.021$).

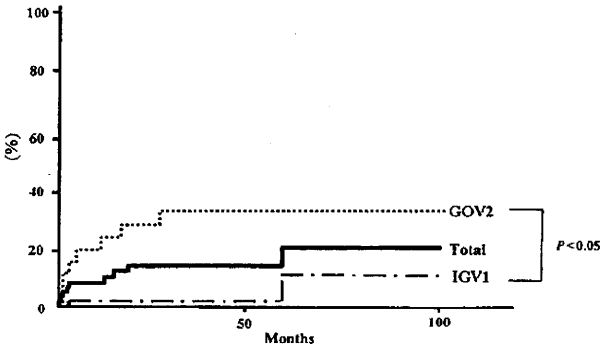


**Figure 5** Cumulative occurrence rate for risky esophageal varices (EVx) after balloon-occluded retrograde transvenous obliteration (B-RTO) (Kaplan–Meier analysis).

EVx at 1, 5 and 8 years was 8.6%, 17.6% and 21.2%, respectively. The cumulative occurrence rate of risky EVx in GOV2 patients was 19.5%, 35.0% and 35.0% at 1, 5 and 8 years, respectively, and that in IGV1 patients was 3.1%, 13.9% and 13.9% at 1, 5 and 8 years, respectively. There was a significant difference in the rate of risky EVx occurrence between GOV2 and IGV1 patients ($P < 0.05$) (Fig. 5).

### PTP assessment

Portal venous pressure was measured in 17 of 68 patients (25%) by PTP during the B-RTO procedure. The average PVP was 31.3 cm $H_2O$ (range, 21.5–41.0). The patients were classified according to PVP. The higher PVP group was defined as PVP greater than 30 cm $H_2O$. Of 17 patients, 10 were included in the higher PVP group. In the B-RTO procedure, patients with higher PVP required more ethanol (lower PVP of 3.5 vs higher of 9.1 mL; $P < 0.05$), but this was not the case for the EOI procedure (lower PVP of 32.8 vs higher PVP of 35.8 mL; $P = 0.69$). As a result, the B-RTO procedure took longer in patients with higher PVP than those with low PVP (45.5 ± 15.1 vs 81.0 ± 25.4 min; $P < 0.05$). Although risky EVx developed in six of 10 patients with higher PVP after B-RTO, it developed in only one of seven patients with lower PVP. Importantly, eight of 10 patients with higher PVP had GOV2. PTP also revealed hemodynamic characteristics of IGV1 and GOV2. Of the 17 cases, nine had GOV2 and eight had IGV1. As shown in Table 3, higher PVP was recognized in six of nine cases (66.7%) with GOV2 and in two of eight cases (25.0%) with GOV1 ($P = 0.185$). The PTP study also revealed that the main inflow route of IGV1-GVx tended to be the short or posterior gastric vein. However, there was no significant difference between GOV2 and IGV1 in PVP and main inflow route of GVx (Table 3).

## Discussion

Although endoscopic injection of cyanoacrylate (Histoacryl) is not ideal, it is currently the only effective method recommended for the treatment of acute gastric variceal bleeding.[20] Some investigators insist that EIS with cyanoacrylate is the best treatment for GVx bleeding.[21–24] In recent reports of the long-term efficacy of cyanoacrylate for GVx bleeding, the hemostasis rates for GVx

**Table 3** Result of percutaneous transhepatic portography assessment

| | GOV2 ($n = 9$) | IGV1 ($n = 8$) |
|---|---|---|
| PVP | | |
| Lower PVP ($n = 9$) | 3 (33.3%) | 6 (75.0%) |
| Higher PVP ($n = 8$) | 6 (66.7%) | 2 (25.0%) |
| | $P = 0.185$ | |
| Main inflow rout | | |
| LGV ($n = 7$) | 5 (55.5%) | 2 (25.0%) |
| SGV or PGV ($n = 10$) | 4 (44.5%) | 6 (75.0%) |
| | $P = 0.334$ | |

GOV2, gastric varices concomitant with esophageal varices; IGV1, gastric varices without esophageal varices; LGV, left gastric vein; PGV, posterior gastric vein; SGV, short gastric vein.

bleeding were 94–97% and the recurrence rates were 21–60%.[21–24] These hemostasis rates seem to be satisfactory; therefore, we previously performed EIS with cyanoacrylate for the hemostasis of active bleeding from GVx.[25] The recurrence rate remained high, however, compared with that of EIS treatment for EVx. Therefore, effective additional therapy with B-RTO is desirable after achieving hemostasis. The present study demonstrated a recurrent bleeding rate of 2/18 (3.2%) in cases with previous bleeding and 0/45 (0%) prophylaxis. Therefore, we believe that B-RTO is a more effective therapy than conventional therapies for preventing GVx bleeding. The present study also demonstrated that prophylactic B-RTO can prevent bleeding of risky GVx over the long term. B-RTO should be used to eradicate risky GVx to avoid bleeding and subsequent life-threatening events.

Transjugular intrahepatic portosystemic shunts are reported to be effective as salvage treatment for EVx.[26] Encephalopathy and shunt occlusion, however, are severe complications that can occur over the long term.[4,27] PVP of patients with GVx is lower than that with EVx because they have a large gastrorenal shunt;[28] therefore, it is likely that TIPS for GVx are less effective than for EVx.[13,27]

Some investigators report that Hassab's operation and portosystemic shunt surgery is the definitive therapy for GVx bleeding. Our previous study also indicated that Hassab's operation for GVx is an effective treatment to prevent initial and recurrent bleeding of GVx over the long term.[14] The choice of the surgical procedure, however, depends on the severity of the liver dysfunction, and patients with GVx bleeding often have poor liver function.[29]

Our B-RTO techniques differ slightly from those used in other facilities. We usually retain the B-RTO catheter until the next morning when the patients are able to walk to the bathroom by themselves. In other reports of B-RTO, Chikamori *et al.*[17] left the catheter in for 2 or 3 days in seven patients (13.4%; 7/52) and Fukuda *et al.*[16] performed repeated B-RTO (two or three times) in 22 patients (44%; 22/50) to obliterate GVx. Our long-term results indicate that a one-time procedure and overnight catheter retention are sufficient to obliterate GVx in most cases. The differences in the results of these procedures seem to be due to whether or not outflow routes were successfully blocked. In the present study, 50% glucose was useful to obstruct the outflow routes. To enhance the obstruction of the outflow collaterals using 50% glucose, the amount of ethanol can be reduced.

Ten patients (17.2%) developed EVx after B-RTO, and three patients bled from EVx that developed after B-RTO. Because esophageal bleeding can occur following B-RTO, we provided close follow up and endoscopic treatment (EIS or endoscopic variceal ligation) prophylactically when risky EVx developed. Therefore, EVx bleeding has not occurred in these patients since 1998. One long-term study of transjugular retrograde obliteration (an alternative B-RTO method) reported that the cumulative occurrence rate of EVx was 36% at 1 year and 56% at 5 years.[17] Another study reported that eight (16.6%) patients had worsening EVx and the cumulative occurrence rate was 2% at 1 year and 12.6% at 5 years.[16] EVx was not a cause of death in these reports. As some investigators have pointed out, ectopic intestinal varices or severe rectal varices, which are difficult to treat, might occur after major shunt closure by B-RTO.[4] In the present study, however, none of the patients suffered ectopic variceal bleeding.

In the B-RTO procedure, patients with higher PVP required more ethanol, but not EOI. This means that patients with GVx and higher PVP have more collaterals requiring ethanol obstruction. Therefore, the B-RTO procedure took longer in patients with higher PVP than those with low PVP. The PTP study revealed that patients with GOV2-Vx tended to have higher PVP and IGV1-Vx tended to be supplied mainly by the short or posterior gastric vein. However, there was no significant difference in PVP and main inflow route of GVx between IGV1 and GOV2. The reason is thought to be that the results were obtained from a study of only a small number of patients. Further hemodynamic studies are necessary to elucidate that difference in more patients.

The cumulative survival rate of patients after B-RTO was 78.1% at 8 years, which seems relatively high. Interestingly, there was no significant difference in the survival rate between Child–Pugh A and B or C classifications. One report of B-RTO indicated that the prognosis of patients without HCC is not affected by the severity of liver dysfunction.[17] Improvement of hepatic function in 1 week to 12 months after B-RTO was also reported.[30,31] Moreover, some investigators demonstrated the possibility of improved hepatic function after an increase in portal blood flow using the rabbit fibrosis model[32] and isolated perfused human livers.[33] Taken together, it is possible that increased portal blood flow due to B-RTO may improve or preserve hepatic function in some cirrhotic patients.

Because we previously encountered two severe complications (pulmonary embolism and ventricular fibrillation) due to using absolute ethanol or a large amount of EOI, we have used 50% glucose to obliterate outflow collaterals over the last 5 years.[34] As a result, we have not encountered such severe complications for the last 5 years.

Balloon-occluded retrograde transvenous obliteration is beneficial, despite worsening EVx, because the effectiveness and improved mortality are excellent compared to our previous results using EIS with Histoacryl.[25] Therefore, we now perform B-RTO as the first treatment for elective and prophylactic treatment (Fig. 6).

In GVx bleeding cases, most rebleeding occurs within 1 year after hemostasis obtained with cyanoacrylate injection;[23–25] thus, additional therapy such as B-RTO should be performed as soon as possible after the general condition is improved after hemostasis.

In conclusion, B-RTO treatment for GVx is a highly effective method to prevent GVx rebleeding and initial bleeding over the long term. Therefore, we propose that B-RTO might be a first-choice radical treatment after hemostasis of GVx bleeding or prophylactic treatment for risky GVx. Further controlled trials, including cost-benefit analysis, are required.

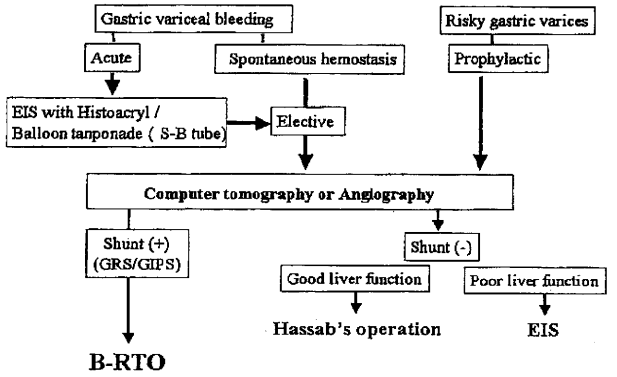


**Figure 6** Schematic diagram showing our strategy for gastric varices (GVx) with active bleeding, such as a spurting or oozing bleeding (acute case), with recent bleeding signs such as clot or fibrin clot (elective case), and with nodular (F2), tumorous (F3) and/or red color on the variceal surface, which are likely to bleed (prophylactic case). Computer tomography or angiography was performed in all patients to determine the existence of a gastrorenal shunt (GRS) or a gastroinferior phrenic shunt (GIPS), for which the balloon-occluded retrograde transvenous obliteration (B-RTO) procedure is indicated.

## References


1 Sarin SK, Lahoti D, Saxena SP *et al.* Prevalence, classification and natural history of gastric varices: a long-term follow-up study in 568 portal hypertension patients. *Hepatology* 1992; **16**: 1343–9.
2 Greig JD, Garden OJ, Anderson JR *et al.* Management of gastric variceal haemorrhage. *Br. J. Surg.* 1990; 77: 297–9.
3 Hashizume M, Kitano S, Yamaga H *et al.* Endoscopic classification of gastric varices. *Gastrointest. Endosc.* 1990; **36**: 276–80.
4 Ryan BM, Stockbrugger RW, Ryan JM. A pathophysiologic, gastroenterologic, and radiologic approach to the management of gastric varices. *Gastroenterology* 2004; **126**: 1175–89.
5 Sorbi D, Gostout CJ, Peura D *et al.* An assessment of the management of acute bleeding varices: a multicenter prospective member-based study. *Am. J. Gastroenterol.* 2003; **98**: 2424–34.
6 Ferguson JW, Tripathi D, Hayes PC. Review article: the management of acute variceal bleeding. *Aliment. Pharmacol. Ther.* 2003; **18**: 253–62.
7 Seewald S, Mendoza G, Seitz U, Salem O, Soehendra N. Variceal bleeding and portal hypertension: has there been any progress in the last 12 months? *Endoscopy* 2003; **35**: 136–44.
8 McCormick PA, O'Keefe C. Improving prognosis following a first variceal haemorrhage over four decades. *Gut* 2001; **49**: 682–5.
9 Imperiale TF, Chalasani N. A meta-analysis of endoscopic variceal ligation for primary prophylaxis of esophageal variceal bleeding. *Hepatology* 2001; **33**: 802–7.
10 Korula J, Chin K, Ko Y, Yamada S. Demonstration of two distinct subsets of gastric varices: Observations during a seven-year study of endoscopic sclerotherapy. *Dig. Dis. Sci.* 1991; **36**: 303–9.
11 Trudeau W, Prindiville T. Endoscopic injection sclerosis in bleeding gastric varices. *Gastrointest. Endosc.* 1986; **32**: 264–8.
12 Kanagawa H, Mima S, Kouyama H *et al.* Treatment of gastric fundal varices by balloon-occluded retrograde transvenous obliteration. *J. Gastroenterol. Hepatol.* 1996; **11**: 51–8.
13 Chau TN, Patch D, Chan YW *et al.* 'Salvage' transjugular intrahepatic portosystemic shunts: gastric fundal compared with esophageal variceal bleeding. *Gastroenterology* 1998; **114**: 981–7.
14 Tomikawa M, Hashizume M, Saku M *et al.* Effectiveness of gastric devascularization and splenectomy for patients with gastric varices. *J. Am. Coll. Surg.* 2000; **191**: 498–503.
15 Kawanaka H, Ohta M, Hashizume M *et al.* Portosystemic encephalopathy treated with balloon-occluded retrograde transvenous obliteration. *Am. J. Gastroenterol.* 1995; **90**: 508–10.
16 Fukuda T, Hirota S, Sugiura K *et al.* Long-term results of balloon-occluded retrograde transvenous obliteration for the treatment of gastric varices and hepatic encephalopathy. *J. Vasc. Interv. Radiol.* 2001; **12**: 327–36.
17 Chikamori F, Kuniyoshi N, Shibuya S *et al.* Eight years of experience with transjugular retrograde obliteration for gastric varices with gastrorenal shunt. *Surgery* 2001; **129**: 414–20.
18 Hashizume M, Kitano S, Yamaga H *et al.* Haptoglobin to protect against renal damage from ethanolamine oleate sclerosant. *Lancet* 1988; **2**: 340–1.
19 Japanese Research Society for Portal Hypertension. The general rules for recording endoscopic findings on esophageal varices. *Jpn. J. Surg.* 1980; **10**: 84–7.
20 de Franchis R. Evolving consensus in portal hypertension. Report of the Baveno IV consensus workshop on methodology of diagnosis and therapy in portal hypertension. (Published erratum in *J. Hepatol.* 2005; **43**: 547.) *J. Hepatol.* 2005 **43**: 167–76.
21 D'Imperio N, Piemontese A, Baroncini D *et al.* Evaluation of undiluted N-butyl-2-cyanoacrylate in the endoscopic treatment of upper gastrointestinal tract varices. *Endoscopy* 1996; **28**: 239–43.
22 Lo GH, Lai KH, Cheng JS *et al.* A prospective, randomized trial of butyl cyanoacrylate injection versus band ligation in the management of bleeding gastric varices. *Hepatology* 2001; **33**: 1060–4.
23 Kind R, Gugkielmi A, Rodella L *et al.* Bucrylate treatment of bleeding gastric varices; 12 years' experience. *Endoscopy* 2000; **32**: 512–9.
24 Huang YH, Yeh HZ, Chen GH *et al.* Endoscopic treatment of bleeding gastric varices by N-butyl-2-cyanoacrylate (Histoacryl) injection: long-term efficacy and safety. *Gastrointest. Endosc.* 2000; **52**: 160–7.
25 Akahoshi T, Hashizume M, Shimabukuro R *et al.* Long-term result of endoscopic histoacryl injection sclerotherapy for gastric variceal bleeding. *Surgery* 2002; **131**: S177–181.
26 Azoulay D, Castaing D, Majno P *et al.* Salvage transjugular intrahepatic portosystemic shunt for uncontrolled variceal bleeding in patients with decompensated cirrhosis. *J. Hepatol.* 2001; **35**: 590–7.
27 Tripathi D, Therapondos G, Jackson E *et al.* The role of the transjugular intrahepatic portosystemic stent shunt (TIPSS) in the management of bleeding gastric varices: clinical and haemodynamic correlations. *Gut* 2002; **51**: 270–4.
28 Watanabe K, Kimura K, Matsutani S *et al.* Portal hemodynamics in patients with gastric varices: A study in 230 patients with esophageal and /or gastric varices using portal vein catheterization. *Gastroenterology* 1988; **95**: 434–40.
29 Kim T, Shijo H, Kokawa H *et al.* Risk factors for hemorrhage from gastric fundal varices. *Hepatology* 1997; **25**: 307–12.
30 Akahane T, Iwasaki T, Kobayashi N *et al.* Changes in liver function parameters after occlusion of gastrorenal shunts with balloon-occluded retrograde transvenous obliteration. *Am. J. Gastroenterol.* 1997; **92**: 1026–30.
31 Miyamoto Y, Oho K, Kumamoto M *et al.* Balloon-occluded retrograde transvenous obliteration improves liver function in patients with cirrhosis and portal hypertension. *J. Gastroenterol. Hepatol.* 2003; **18**: 934–42.
32 Cardoso JE, Giroux L, Assisi I *et al.* Liver function improvement following increased portal blood flow in cirrhotic rats. *Gastroenterology* 1994; **107**: 460–7.

33 Jiao LR, Seifalian AM, Habib N, Davidson BR. The effect of mechanically enhancing portal venous inflow on hepatic oxygenation, microcirculation, and function in a rabbit model with extensive hepatic fibrosis. *Hepatology* 1999; **30**: 46–52.

34 Chang KY, Wu CS, Chen PC. Prospective, randomized trial of hypertonic glucose water and sodium tetradecyl sulfate for gastric variceal bleeding in patients with advanced liver cirrhosis. *Endoscopy* 1996; **28**: 481–6.

*The American Journal of Pathology, Vol. 175, No. 2, August 2009*

*DOI: 10.2353/ajpath.2009.081061*

*Gastrointestinal, Hepatobiliary and Pancreatic Pathology*

# Endothelial to Mesenchymal Transition via Transforming Growth Factor-β1/Smad Activation Is Associated with Portal Venous Stenosis in Idiopathic Portal Hypertension

Azusa Kitao,*† Yasunori Sato,* Seiko Sawada-Kitamura,* Kenichi Harada,* Motoko Sasaki,* Hiroyasu Morikawa,‡ Susumu Shiomi,§ Masao Honda,¶ Osamu Matsui,† and Yasuni Nakanuma*

*From the Departments of Human Pathology,* Radiology,† and Gastroenterology,¶ Kanazawa University Graduate School of Medicine, Kanazawa; and the Departments of Hepatology,‡ and Nuclear Medicine,§ Osaka City University Graduate School of Medicine, Osaka, Japan*

**Idiopathic portal hypertension (IPH) represents noncirrhotic portal hypertension of unknown etiology, mainly due to stenosis of peripheral portal veins. This study was performed to clarify the mechanism of portal venous stenosis in IPH from the viewpoint of the contribution of the endothelial to mesenchymal transition of the portal vein endothelium via transforming growth factor-β1 (TGF-β1)/Smad activation. *In vitro* experiments using human dermal microvascular endothelial cells demonstrated that TGF-β1 induced myofibroblastic features in human dermal microvascular endothelial cells, including spindle cell morphology, reduction of CD34 expression, and induction of S100A4, α-smooth muscle actin, and COL1A1 expression, as well as the increased nuclear expression of phospho-Smad2. Bone morphogenic protein-7 preserved the endothelial phenotype of human dermal microvascular endothelial cells. Immunohistochemical analysis showed that endothelial cells of the peripheral portal veins in IPH were characterized by the decreased expression of CD34 and the enhanced nuclear expression of phospho-Smad2; these results also confirmed the expression of S100A4 and COL1A1 in the portal vein endothelium. Serum TGF-β1 levels in patients with IPH were significantly higher than those of healthy volunteers and patients with chronic viral hepatitis/liver cirrhosis, while an elevation of serum bone morphogenic protein-7 levels was not observed. These results suggest that the endothelial to mesenchymal transition of the portal venous endothelium via TGF-β1/Smad activation is associated with portal venous stenosis in IPH, and bone morphogenic protein-7 may therefore be a suitable therapeutic candidate for IPH. *(Am J Pathol 2009, 175:616–626; DOI: 10.2353/ajpath.2009.081061)***

Idiopathic portal hypertension (IPH) is a condition of noncirrhotic presinusoidal portal hypertension of unknown etiology, primarily affecting adults.[1–3] Clinical presentations of IPH include splenomegaly, pancytopenia, gastroesophageal varices, and subcapsular parenchymal atrophy of the liver.[1] Histologically, phlebosclerosis and stenosis of peripheral portal veins associated with dense portal fibrosis are common and characteristic findings of IPH, accounting for portal hypertension due to presinusoidal block.[4–6] Hepatic function tends to be well preserved even at an advanced disease stage, but hepatic failure can lead to fatal outcome in some patients.[7] To date, a radical treatment is not available other than liver transplantation,[8,9] because the mechanism of portal venous stenosis of IPH has not been clarified.

IPH in patients is reported to be complicated with collagen vascular diseases such as systemic sclerosis.[10,11] Systemic sclerosis is a disease that causes excessive collagen production and deposition, vascular damage, and inflammation in multiple organs including skin, lung, and the gastrointestinal tracts.[12] Patients with

Supported by the Japanese Study Group of Intrahepatic Hemodynamics Alterations (Chairmen: Professor Makoto Hashizume, Kyushu University Graduate School of Medicine, Fukuoka; Professor Fuminori Moriyasu, Tokyo Medical School, Tokyo, Japan).

A.K. and Y.S. contributed equally to this work.

Accepted for publication May 5, 2009.

Address reprint requests to Yasuni Nakanuma, MD, PhD, Department of Human Pathology, Kanazawa University Graduate School of Medicine, 13-1 Takara-machi, Kanazawa 920-8640, Japan. E-mail: pbcpsc@kenroku.kanazawa-u.ac.jp.

the disease show an increased deposition of collagen types I and III in various organs, with type I being the most abundant.[12] Transforming growth factor-β (TGF-β) contributes greatly to the fibrotic processes, and elevation of circulating TGF-β level has been reported in patients with systemic sclerosis.[13,14] Although excessive collagen deposition in systemic sclerosis appears to be mediated by complex networks of various factors, one possible mechanism of the cutaneous fibrogenesis is that dermal microvascular endothelial cells transform into myofibroblastic cells, thereby contributing to the collagen deposition in the dermis.[15,16]

Recently, it has been described with increasing frequency that vascular endothelial cells have an ability to acquire matrix-producing myofibroblastic features, providing proof of principle for the process of endothelial to mesenchymal transition (EndMT).[17–19] EndMT is a phenomenon reported to occur during embryonic cardiovascular development,[20,21] and also occur under several pathological conditions including cardiac fibrosis and carcinoma-associated interstitial fibrosis.[17,18] EndMT is a phenotypic conversion characterized by the down-regulation of vascular endothelial markers such as CD31 and von Willebrand factor, and the emergence of myofibroblastic markers such as S100A4/fibroblast-specific protein-1 and α-smooth muscle actin (α-SMA).[16–18] TGF-β1 acts as a potent inducer of EndMT both *in vitro* and *in vivo*.[17,18,20]

TGF-β binds to TGF-β receptor type II (TβR-II), and it recruits the TGF-β receptor type I (TβR-I). TβR-I subsequently phosphorylates Smad2 and Smad3, which form hetero-oligomers with Smad4. They translocate from the cytoplasm to the nucleus, where they regulate transcription of target genes.[22] Bone morphogenic protein-7 (BMP7) is a member of the TGF-β superfamily, and a promising TGF-β antagonist.[23,24] BMP7 binds and activates BMP type II receptor that subsequently form complex with BMP receptor type IA. The receptors activated by BMP7 phosphorylate Smad1, 5 and 8, which counteract Smad2/3 phosphorylation by TGF-β. Indeed, BMP7 has been shown to inhibit EndMT in a mouse model of cardiac fibrosis.[17]

In most types of chronic liver disease, hepatic fibrosis is mediated by myofibroblasts, which generally originate from hepatic stellate cells. Portal fibroblasts and bone-marrow derived fibrocytes are other candidates of cell types of myofibroblast precursor in the liver.[25] Given the facts that systemic sclerosis is a clinical complication of IPH, and EndMT is one of the possible causative mechanism of excessive collagen deposition in systemic sclerosis, it is plausible that, in IPH, stenosis of peripheral portal veins with dense collagenous fibrosis around them is mediated by EndMT of the endothelial cells of portal vein, and the endothelial cell may be another contributor of the portal fibrosis.

To clarify this, the involvement of EndMT in portal venous stenosis of IPH was examined by the use of microvascular endothelial cells *in vitro*, and by means of histological analysis using liver tissue sections of IPH. Measurement of the serum TGF-β1 and BMP7 levels was also performed using samples obtained from IPH patients.

## Materials and Methods

This human study was performed with the approval of the ethics committee of Kanazawa University Graduate School of Medicine.

### Cell Culture

Human dermal microvascular endothelial cells (HMVEC) were purchased from Cell Applications, Inc. (San Diego, CA), and were maintained with endothelial growth medium (CADMEC growth medium, Cell Applications, Inc.). HMVECs were then treated with either TGF-β1 (10 ng/ml; R&D systems, Inc., Minneapolis, MN) alone or in combination with BMP7 (up to 100 ng/ml; R&D systems, Inc.) for 5 days, and phenotypic changes of HMVECs were examined as described below. Experiments were conducted with HMVECs at passages 2 to 4.

### Reverse Transcription-PCR and Quantitative Real-time PCR

Reverse transcriptase (RT) PCR was performed using total RNA (1 μg) extracted from HMVECs. Total RNA was extracted using an RNA extraction kit (RNeasy mini; Qiagen, Tokyo, Japan) and was used to synthesize cDNA with reverse transcriptase (ReverTra Ace; Toyobo Co., Osaka, Japan). The sequences of the primers and conditions for PCR used are shown in Table 1. The PCR products were subjected to 2% agarose gel electrophoresis and stained with ethidium bromide.

Quantitative real-time PCR was performed according to a standard protocol using the SYBR Green PCR Master Mix (Toyobo Co.) and ABI Prism 7700 Sequence Detection System (PE Applied Biosystems, Warrington, UK). Cycling conditions were incubation at 50°C for 2 minutes, 95°C for 10minutes, and 40 cycles of 95°C for 15 seconds and 60°C for 1 minute. Fold difference compared with glyceraldehyde-3-phosphate dehydrogenase expression was calculated.

### Western Blot Analysis

Total proteins were extracted from HMVEC using T-PER protein extraction reagent (Pierce Chemical Co., Rockford, IL). First, 5 μg of the protein was subjected to 10% SDS-polyacrylamide gel electrophoresis, and then electrophoretically transferred on to a nitrocellulose membrane. The membrane was incubated with primary antibodies against CD31 (1:200, JC70A, mouse monoclonal; DakoCytomation, Glostrup, Denmark), CD34 (1:250, QBEND10, mouse monoclonal; Immunotech, Marseilles, France), S100A4 (1:200, rabbit polyclonal; Abcam Inc., Cambridge, MA), α-SMA (1:200, 1A4, mouse monoclonal; DakoCytomation), pro-COL1A1 (1:200, goat polyclonal, Santa Cruz Biotechnology, Inc., Santa Cruz, CA), and actin (1:3000, AC-15, mouse monoclonal; Abcam

**Table 1.** Sequences of the Primers and PCR Conditions Used in this Study

| Gene | Sequences | Annealing temperature (°C) | PCR cycles | Product size (bp) |
|---|---|---|---|---|
| *TβR-I* | 5′-GGCCATTTACACTGAATGAG-3′<br>5′-GGCTTAGAAATGGCCCAAAA-3′ | 55 | 40 | 386 |
| *TβR-II* | 5′-GTGGAGACACTTACAAAGCT-3′<br>5′-GAAACTTGGGCTAACTGAGA-3′ | 55 | 40 | 250 |
| *BMP-RIA* | 5′-GGTTTCATAGCGGCAGACAT-3′<br>5′-CTTTCCTTGGGTGCCATAAA-3′ | 55 | 40 | 198 |
| *BMP-RII* | 5′-GCTAAAATTTGGCAGCAAGC-3′<br>5′-CTTGGGCCCTATGTGTCACT-3′ | 55 | 40 | 224 |
| *CD31* | 5′-CCTGCTAAGTTAATGTTGGG-3′<br>5′-GAAAAAACCAGCCTCTAACC-3′ | 62 | 40 | 269 |
| *CD34* | 5′-CCAATCTGACCTGAAAAAGC-3′<br>5′-CCACCGTTTTCCGTGTAATA-3′ | 55 | 30 | 216 |
| *S100A4* | 5′-GGTGACAAGTTCAAGCTCAA-3′<br>5′-CTGGGAAGCCTTCAAAGAAT-3′ | 55 | 40 | 214 |
| *α-SMA* | 5′-GAAATGAACGTTTCCGCTGC-3′<br>5′-CAGACAGAGTATTTGCGCTC-3′ | 62 | 40 | 268 |
| *COL1A1* | 5′-GTCTTCTGCAACATGGAGAC-3′<br>5′-CAGTGGTAGGTGATGTTCTG-3′ | 62 | 40 | 245 |
| *GAPDH* | 5′-GAGTCAACGGATTTGGTCGT-3′<br>5′-TTGATTTTGGAGGGATCTC-3′ | 55 | 30 | 240 |

Inc.). The protein expression was detected using an EnVision+ system (DakoCytomation) and a HISTOFINE system (Nichirei, Tokyo, Japan). 3,3′-diaminobenzidine tetrahydrochloride was used as the chromogen. Semiquantitative analysis of the results was performed using NIH J image software (National institutes of Health, Bethesda, MD). The fold difference compared with actin expression was calculated.

## *Immunocytochemistry*

HMVECs were fixed with 4% paraformaldehyde for 15 minutes, and permeabilized for 3 minutes with 0.1% Triton X-100. After blocking, the cells were incubated for 1 hour at room temperature with primary antibodies against CD34 (1:200, Immunotech), S100A4 (1:100, Abcam Inc.), α-SMA (DakoCytomation), pro-COL1A1 (1:100, goat polyclonal, Santa Cruz Biotechnology, Inc.), and phospho-Smad2 (pSmad2) (1:100, Ser465/467, rabbit polyclonal; Cell Signaling Technology, Inc., Danvers, MA). The protein expression was detected using the alkaline phosphatase-labeled polymer, the HISTOFINE system (Nichirei). Color development was performed using the Vector Red alkaline phosphatase substrate kit (Vector Laboratories, Burlingame, CA), and nuclei were stained with 4′6-diamidino-2-phenylindole. The signals were detected under immunofluorescence confocal microscopy.

## *Liver Specimens*

A total of 44 liver specimens were used. Twenty-four specimens corresponded to IPH. Clinicopathological features of IPH cases were summarized in Table 2. Both liver biopsy and autopsy materials were included. The IPH livers of autopsy cases were collected as previously described, and all autopsy livers were obtained at an advanced disease stage corresponding to Stage III or Stage IV.[1,7] Histology of the liver confirmed the diagnosis of IPH, and five cases corresponded to incomplete septal cirrhosis. Complication of systemic sclerosis was observed in three cases.

As controls, liver specimens obtained from patients with chronic viral hepatitis/liver cirrhosis (CVH/LC) ($n$ = 10), and histologically normal livers (NL) ($n$ = 10) were used. The causes of CVH/LC were viral infection of hepatitis B ($n$ = 2) and hepatitis C ($n$ = 8). NL specimens were obtained from patients undergoing a partial hepatectomy for the diseases other than hepatobiliary disorders such as metastatic colon cancer, and macroscopically and microscopically normal areas were used.

## *Immunohistochemistry*

Liver specimens were fixed with neutral formalin, and 4-μm thick paraffin-embedded tissue sections were pre-

**Table 2.** Clinicopathological Features of IPH Cases Used for Histological Analysis

| *N* | Age (years) | Sex (male:female) | Specimen (biopsy:autopsy) | Splenomegaly | Esophageal varices | Liver weight* (g) | Splenic weight* (g) | Liver fibrosis† | Systemic sclerosis |
|---|---|---|---|---|---|---|---|---|---|
| 24 | 59 ± 20 | 7:17 | 6:18 | 22(92%) | 17(77%) | 779 ± 293 | 378 ± 176 | 5(21%) | 3(13%) |

*Liver and splenic weight were the value of autopsy cases.
†Liver fibrosis corresponded to incomplete septal cirrhosis.